

**"Workshop on Three-Dimensional Modelling  
of Seismic Waves Generation and their Propagation"**

**25 September - 6 October 2000**

**RUPTURE DYNAMICS IN 3-D: a REVIEW**

*Raul Madariaga*

Laboratoire de Géologie,  
Ecole Normale Supérieure  
Paris, France



# Rupture Dynamics in 3-D: a Review

Raul Madariaga, Sophie Peyrat

Laboratoire de Géologie, Ecole Normale Supérieure,  
24 rue Lhomond, 75231 Paris Cedex 05, France.

and

Kim B. Olsen

Institute for Crustal Studies, University of California,  
Santa Barbara, USA

September 5, 2000

## Abstract

We review some recent results on the propagation of seismic ruptures along a planar fault surface subject to a friction law that contains a finite length scale and therefore has a well defined fracture energy flow. For this study we use the new fourth order finite difference method developed by Olsen, Madariaga and Archuleta. We look first at the rupture of an unbounded fault plane starting from a single circular asperity. Rupture propagation is simple but presents substantial differences with the self-similar shear crack model of Kostrov: the most important being that ruptures do not have circular symmetry because rupture resistance can never be uniform around the edge of the rupture front. We study the non-linear parameterization of this problem and show that there is a simple non-dimensional parameter  $\kappa$  that controls the overall properties of rupture propagation. This number generalizes previous studies in 2-D and 3-D by Andrews, Das and Aki, Day, Burridge and many others. We demonstrate for several models that the rupture process has a bifurcation point at a critical value  $\kappa = \kappa_c$ , so that for values of  $\kappa$  less than critical rupture does not grow, while for values barely above critical ruptures grow indefinitely at sub-Rayleigh or sub-shear speeds. For values of  $\kappa$  larger than  $1.5 \kappa_c$  an additional bifurcation occurs: rupture in the in-plane direction becomes super-shear and the rupture front develops a couple of “ears” in the in-plane direction. Finally we study a realistic stress distribution derived from the inversion of the accelerograms of the Landers earthquake. This earthquake started from a critical patch that was probably a few km in radius and then rupture evolved under the control of stress and strength heterogeneities. We find that rupture in Landers occurred for a value of  $\kappa$  that was barely above critical, which is the reason rupture was sub-shear on the average. In the presence of stress or strength heterogeneity, rupture propagation becomes very complex and it propagates only in those regions where preexisting stress is high over relatively broad zones. Thus, rupture is a sort of percolation process controlled by the ratio of local available energy to energy release rate.

## Introduction

A number of recent near field studies of well-recorded earthquakes suggest that these events were complex at all scales. The first evidence of these complexities were discussed by Das and Aki (1977), Day (1982) and many others. Beroza and Mikumo (1996), Bouchon (1997), Ide and Takeo (1997) among others showed that stress drop distributions of all well recorded earthquakes were highly variable in space. These properties were interpreted more than 20 years ago in terms of the so-called “asperity” model of Kanamori and Stewart (1978), and the “barrier” model of Das and Aki (1977) who realized that the

uniform dislocation models used at that time lacked some essential features of the earthquake process. Madariaga (1979) showed that seismic radiation from these two models was very similar so that we could not expect to distinguish between them from purely seismological information.

The study of more complex fault models has gained new attention following the suggestion by Carlson and Langer (1979) that earthquakes may become spontaneously complex due to non linear effects in friction. A different view of the origin of complexity was discussed by Rice (1993), Rice and Ben-Zion (1996) and Shaw and Rice (2000) who suggested that at least some of the complexity found by Carlson and Langer might have been due to the lack of a continuum limit in the velocity weakening friction law. They suggested that heterogeneity was probably due to geometrical complexity of fault surfaces. Using a simple regularization of a velocity weakening friction law, Cochard and Madariaga (1996) found that heterogeneity appears spontaneously in well-posed dynamic faulting models only for very strong rate-weakening. More recently, Shaw and Rice (2000) studied the conditions for the development of complexity in well-posed numerical simulations reaching similar conclusions: heterogeneity appears spontaneously only in a limited parameter range.

Thus, although it is not clear at present what the origin of complexity is, earthquakes appear to be complex at all scales shorter than the characteristic length scale of the fault (the wavelength associated with the corner frequency). As proposed by Bak et al (1987) such a pervasive complexity must be due to the spontaneous organization of the fault in a situation close to criticality. The earthquake model proposed by Bak et al (1987) based on the simplified dynamics of a sand pile, was not very realistic because it lacked radiation, stress drop was immediately recovered inside the fault, etc.

In order to settle the question of why most earthquakes are complex we must model them accurately, taking into account all the relevant length scales in the problem, both (intrinsic) length scales associated with friction as well as (extrinsic) length scales associated with fault size and asperity distribution. This is not a simple task because accurate numerical modeling of ruptures requires large amounts of computer resources. Das and Kostrov (1983) and Day (1982) made calculations of complex faults with heterogeneous distributions of stress and rupture resistance, but these models did not have enough resolution to study the more difficult problem of the interaction between intrinsic and extrinsic length scales. Recent development of finite difference methods in 3-D (Harris and Day, 1994; Mikumo and Miyatake, 1995; Olsen et al, 1997), or boundary Integral Equation methods (Fukuyama and Madariaga, 1997) together with the availability of fast parallel computers has opened the way to the study of accurate dynamic rupture propagation models.

In this paper we first review the properties of three dimensional rupture propagation for two simple classical models of rupture: (1) rupture of an unbounded fault plane starting from a localized asperity; and (2) rupture of a shallow rectangular strike slip fault. From the review of the properties of these models we suggest that rupture propagation is controlled by a simple non-dimensional number that we call  $\kappa$ . This non-dimensional number has a critical value below which ruptures either do not propagate at all or die very quickly. For values of  $\kappa$  slightly above critical, ruptures grow at speeds close to the shear wave speed as most earthquakes do; while for larger values ruptures grow faster than the speed of shear waves, something that is rarely observed in earthquakes. By examining the stress field of the Landers earthquake of June 1992, we suggest that rupture occurred at non-dimensional numbers that was very close to critical.

## Modeling complex earthquakes in 3-D

We study rupture propagation along a planar fault plane embedded in a heterogeneous elastic isotropic medium. The elastic properties of the earth model may be heterogeneous, include a free surface, etc. We use the velocity stress formulation of elastodynamics (Madariaga, 1976) which we rewrite here for

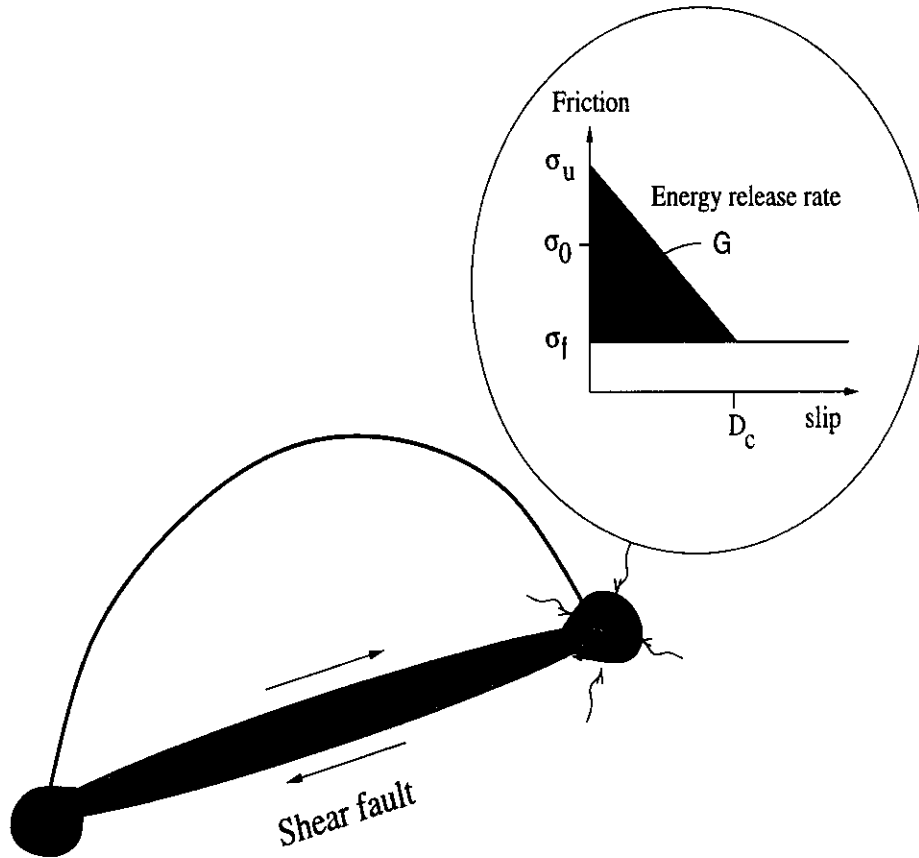


Figure 1: Geometry of a simple rupture propagating along a flat fault embedded in a 3-D elastic medium. Rupture propagation is controlled by energy flow into the rupture front. This energy is provided by elastic energy release in the surrounding medium. The boundary conditions on the fault are controlled by friction inside the fault. We use a simple slip weakening friction of peak stress  $T_u$ , slip weakening distance  $D_c$ , and energy release rate  $G$ .

reference:

$$\rho \dot{v}_i = \frac{\partial \sigma_{ij}}{\partial x_j} + f_i \quad (1)$$

$$\dot{\sigma}_{ij} = \lambda \frac{\partial v_i}{\partial x_i} \delta_{ij} + \mu \left[ \frac{\partial v_i}{\partial x_j} + \frac{\partial v_j}{\partial x_i} \right] + \dot{m}_{ij}, \quad (2)$$

where  $v_i$  and  $\sigma_{ij}$  are the particle velocity and stress tensor, respectively.  $\rho$  is density, and  $\lambda, \mu$  are the elastic moduli which can be spatially varying.  $f_i$  is a distribution of body forces and  $m_{ij}$  is the distribution of moment tensor sources. Dots denote differentiation with respect to time. In our model we assume  $f$  to be zero everywhere and the moment tensor density is computed numerically from the solution of frictional boundary conditions.

Earthquake rupture propagation is entirely controlled by the properties of friction between the sides of the fault. In this paper we study rupture propagation along a planar fault that we choose along the plane  $z = 0$ . Friction controls the initiation, development of rupture and the healing of faults. Laboratory experiments at low slip rates were reviewed by Dieterich (1978), who proposed models of rate- and state-dependent friction, and by Ohnaka and Shen (1999) who concluded that their experiments could be explained with a simpler slip-weakening friction law. Actually, from the point of view of earthquake dynamics, these two models of friction are equivalent (Okubo, 1987). Because of the equivalence of the friction laws at high slip rates, we used a simple slip weakening friction law in which slip is zero until the total stress reaches a peak value (yield stress) that we denote with  $\sigma_u$ . Once this stress has been reached, slip  $D$  starts and  $T(D)$  decreases until it reaches a residual, or kinematic friction  $\sigma_f$ :

$$\begin{aligned} T(D) &= T_u \left( 1 - \frac{D}{D_c} \right) + \sigma_f & \text{for } D < D_c, \\ T(D) &= \sigma_f & \text{for } D > D_c, \end{aligned} \quad (3)$$

where  $D_c$  is a characteristic slip distance and  $T_u = \sigma_u - \sigma_f$ . This triangular cohesive friction law was first proposed by Ida (1972) and has been used in numerical simulations of rupture by Andrews (1976), Day (1982) and many others. Without loss of generality, and for ease of our presentation, we will measure all stresses with respect to the residual frictional level  $\sigma_f$ . This is equivalent to assuming that  $\sigma_f = 0$  in (3).

The most important feature of the cohesive friction law (3) is that in order to propagate rupture along the fault plane the elastic medium surrounding the fault has to provide a fracture energy per unit surface of

$$G = \int_0^{D_c} T(D) dD = \frac{1}{2} T_u D_c. \quad (4)$$

Let us remark that slightly different definitions of  $G$  have appeared in the literature. Ida (1972) and Andrews (1976, 1985), for instance, used a  $G$  of 1/2 the value defined in (4).

We solve (1) together with the friction boundary conditions (3) in an elastic medium with radiation conditions at infinity and an initial stress field. Rupture can only occur if the fault is loaded by a preexisting shear stress field. This initial stress field  $\sigma_{zz}^0(x, y, z)$  includes both tectonic loading and the residual stress field left from previous earthquakes on the fault or neighboring ones. Clearly, tectonic stresses are smooth because the loading occurs at large distances from the fault, while stress heterogeneities due to previous earthquakes will be in general of shorter wavelength.

Figure 1 shows the geometry of the fault model we study. The most important feature of the friction law (3) is slip weakening that occurs near the rupture front inside a so-called break-down or cohesive

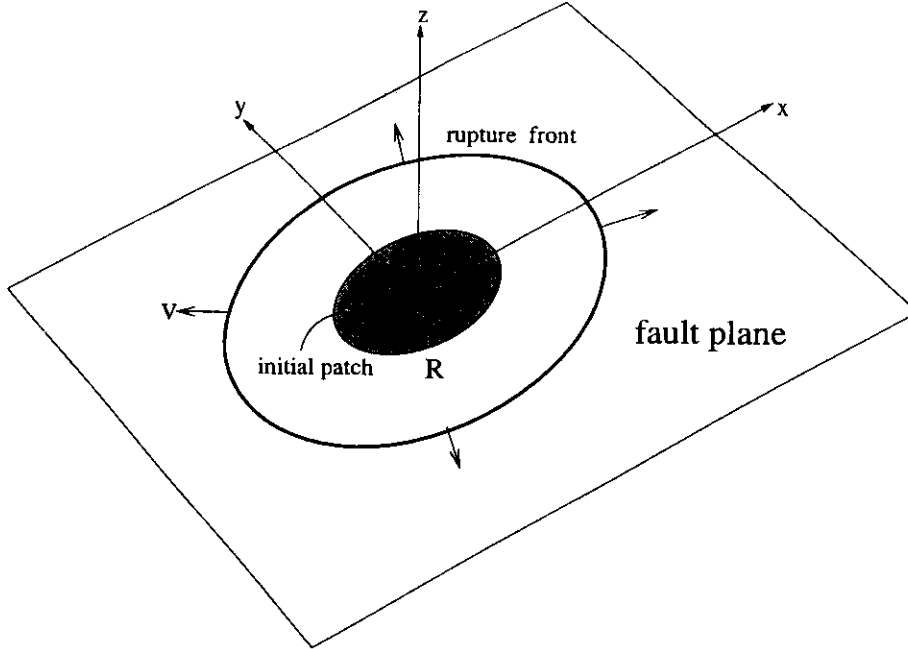


Figure 2: Model of rupture of an unbounded planar fault starting from a localized asperity of circular shape of radius  $R$  that is ready to break.

zone just behind the rupture front. The propagation of the rupture front is completely controlled by the friction law and the distribution of initial stress on the fault.

An essential requirement for the study of dynamic faulting is an accurate and robust method for the numerical modeling of seismic sources. In our recent work we have used a fourth-order formulation of the velocity-stress method (Madariaga, 1976; Olsen et al, 1997; and Madariaga et al., 1998) for the simulation of dynamic rupture propagation on a planar shear fault embedded in a heterogeneous elastic half space. The most important parameter in finite difference modeling of wave propagation is the Courant-Friedrichs-Lewy constant  $H = v_s \Delta t / \Delta x$ , the ratio between temporal and spatial steps. Here  $v_s$  is the shear wave speed. We systematically use  $H \cong 0.2$  in our calculations. We refer to the previously cited papers for further discussion of the numerical method.

## Rupture propagation on a planar uniform fault

We study the spontaneous propagation of rupture along a planar fault subject to a slip weakening friction law (3). It is well known that in order to initiate rupture in such a model an initial high stress patch must be ready to break (Andrews, 1976). Although this model was studied by Das (1981), Day (1982) and Das and Kostrov (1983) we will review it here in order to identify the bifurcations that occur in this problem and the control parameter that determines the generic qualitative properties of rupture dynamics.

### Basic features of spontaneous rupture of a uniform fault

In this section we study spontaneous rupture of a planar fault starting from a circular asperity of radius  $R$  that is ready to break, i.e. it is loaded with stress that is just slightly larger than the peak stress  $T_u$ , and is surrounded by an unbounded fault surface loaded at a constant effective stress level

( $T_e < T_u$ ) as shown in Fig. 2. Friction (3) is uniform everywhere on the fault plane. This is certainly the simplest realistic model of an earthquake. Since we are mainly interested in the parameters that control rupture propagation we did not include any stopping mechanism. It is usually assumed that the Kostrov (1964) solution for a self-similar elliptical fault is an adequate model of this problem and has been used extensively in the literature to simulate the initial radiation from a seismic source (Sato and Hirasawa, 1972, Madariaga, 1976). In fact this model can not be correct for the following reasons:

1. A rupture that grows self-similarly from its origin has no initial energy concentration. As Andrews (1976a,b) and many other authors noted, in order for rupture to initiate, stress must be high over a finite zone, sometimes called the minimum rupture patch. Once rupture has broken the initial zone it will grow or stop depending on the values of the stress field inside ( $T_u$ ) and outside the asperity ( $T_e$ ), and the friction law (3).

2. As shown by Das (1981) and Day (1982), rupture shape can not be circular because, as already pointed by Kostrov (1964), energy release rate in the in-plane direction (mode II) and in mode III are different. Kostrov (1964) proposed that at low speeds ruptures should elongate in the antiplane direction a feature that has been observed in all numerical simulations of three dimensional faults. Additional discussion of this can be found in Fig. 5.14 of Kostrov and Das (1989).

An additional interesting phenomenon, observed in most well resolved numerical simulations, is that for certain values of the parameters ruptures become elongated in the inplane direction and eventually become supershear. Andrews (1976b, 1985), Freund (1988) showed that in-plane 2-D faults may become supershear by a very interesting mechanism where rupture literally jumps ahead of the shear wave speed by the generation of a secondary rupture front that leads the initial rupture at a supershear speed. After a short while the two ruptures coalesce and a single supershear rupture propagates. This important behavior of shear faulting on a prescribed rupture surface has recently been confirmed experimentally by Rosakis et al (1999).

### Numerical simulation of rupture starting from a circular asperity

There seems to be no way to obtain analytical solutions for shear rupture propagation in 3-D analytically, so that even for the simplest problems we have to resort to numerical simulation. In order to gain insight into the behavior of rupture in a well posed problem, we review the very simple problem described in Figure 2. A small circular asperity of finite radius  $R$  breaks suddenly at time  $t = 0$  triggering the propagation of rupture on a uniform unbounded planar fault. This problem has been studied by a large number of authors including Das (1981), Day (1982), Virieux and Madariaga (1982), Das and Kostrov (1983), etc. It is interesting because we will find all the features discussed above. We perform our computations in non-dimensional units such that stresses are scaled by

$$\sigma = T_e \sigma', \quad (5)$$

where we recall that  $T_e$  is the effective stress (average stress drop) and  $\sigma'$  is the non-dimensional stress. Displacements  $u$  are scaled by

$$u = \frac{T_e}{\mu} R u', \quad (6)$$

where  $u'$  is the non-dimensional displacement, and  $R$  is the size of the initial rupture patch that is loaded to the peak stress  $T_u$  and is therefore ready to break. Following (6), particle velocities scale like  $T_u/\mu v_s$ .

In the numerical simulations we fixed the radius of the initial asperity to  $R=18$  grid intervals  $\Delta x$ . As mentioned earlier, the time step was  $\Delta t = 0.2\Delta x/v_s$  where  $v_s$  is the shear wave speed. All other quantities are non-dimensional, so that the peak stress  $T_u = 1$ , the elastic constants  $\lambda = \mu = 1$ ,  $\rho = 1$  and  $v_s = 1$ . We fixed the slip weakening distance  $D_c = 8$  and we let  $T_e$  vary from 0.4 to 0.9.



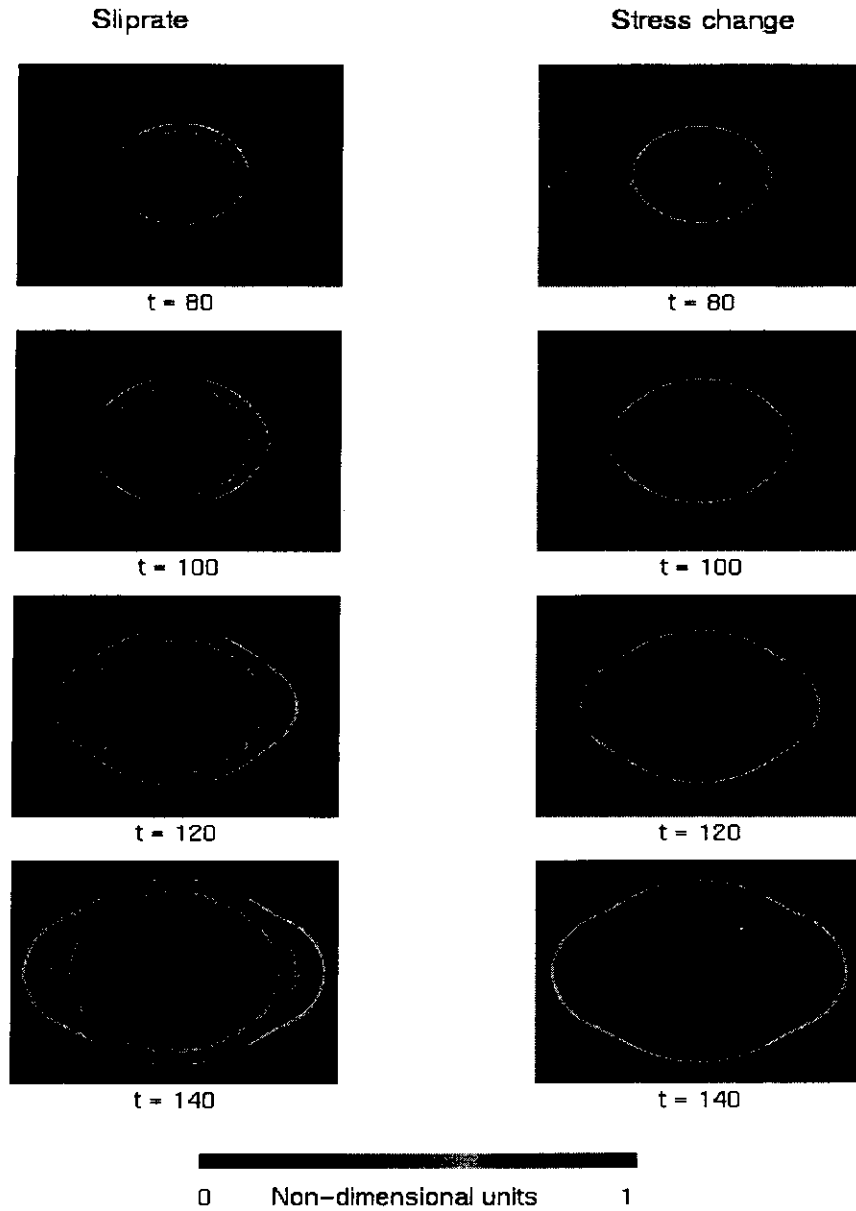


Figure 3: Rupture growth on a flat uniform fault embedded in a homogeneous elastic medium. Rupture starts from a finite initial asperity and then grows at subsonic speed in all spatial directions. After a while rupture along the inplane direction (horizontal direction) jumps at a speed that is higher than that of shear waves. The snapshots on the left show slip rate on the fault; and on the right hand the corresponding shear stress field. Snapshots are shown at four successive instants of time. Time is measured in units of time for a shear wave to cross the asperity. Slightly after time 100, rupture jumps to the super shear speed along the in-plane direction.

In Figure 3 we show as an example the result of the numerical simulation for an effective stress  $T_e = 0.75$ . This figure illustrates most of the important features that are observed in the modeling of simple rupture on unbounded fault surfaces. Initially, rupture starts from the initial circular asperity and accelerates rapidly becoming elongated in the in-plane direction (the horizontal direction in the Figure). At time  $t = 100\Delta t$ , the second row in Figure 3, we observe a certain diffusion of the rupture front near the in-plane direction. This is the onset of the super-shear instability. At times greater than 100 ( $t = 120\Delta t$  and  $t = 140\Delta t$ ), the rupture front acquires an elliptical shape with two protrusions (we call them “ears”) elongated in the in-plane direction (see the bottom snapshots in Figure 3). The transition from subshear to supershear rupture in 3-D is different from that studied by Andrews (1976b, 1985), Das and Aki (1977) and Burridge et al (1979). The rupture front in 3-D does not jump ahead of the S wave as in 2-D, rather it becomes initially unstable along the in-plane direction and then the instability propagates laterally along the rupture front. There is no discontinuity of the rupture front and, at least at the level of resolution that we currently have, we do not observe regions where slip is arrested temporarily between the arrival of the supershear and sub-shear rupture fronts. We observe clearly that there is a peak in slip-rate associated with the super-shear front; and another associated with the older subsonic front. Slip rate decreases between the two fronts, but it does not decrease to zero as in Andrews (1976) in-plane rupture simulations. It is clear that the study of the transition between sub-Rayleigh and super-shear propagation will definitely require much more detailed numerical work.

As suggested by Madariaga and Olsen (2000) it is convenient to interpret the results obtained from numerical experiments in terms of a single non-dimensional parameter that we define as

$$\kappa = \frac{T_e^2 R}{\mu T_u D_c}. \quad (7)$$

This non-dimensional number contains all the relevant parameters for the rupture of an asperity on an unbounded fault plane: the two dimensions  $R$  and  $D_c$  and the two stresses  $T_u$  and  $T_e$ . There are no other free parameters in the problem illustrated in Fig 2. In Figure 3  $\kappa = 1.26$ , a value that is large enough in order to obtain a super-shear transition.

We determined the behavior of rupture as a function of the non-dimensional number  $\kappa$ . For that purpose we fixed all the parameters except  $T_e$  that we made vary from 0.4 to 0.9. As in the example of Fig. 3 the radius of the initial patch was  $R = 18\Delta x$ , time step was  $\Delta t = 0.2\Delta x/v_s$  where  $v_s = 1$  is the shear wave speed. We fixed  $T_u = 1$ ,  $D_c = 8\Delta x$  and  $\mu = 1$ . In Figure 4 we show snapshots of the slip rate (left hand side panels) and shear stress fields on the fault (right hand side panels) computed at the same instant of time,  $t = 120 \Delta x/v_s = 6.66 R/v_s$ , for different values of  $\kappa$ . In the top panel, for  $\kappa = 0.54$  rupture did not succeed in propagating beyond the initial asperity, the activity observed in the slip velocity plot is due to waves propagating inside the still open asperity. The stress field shown on the right hand of the top panel is not completely settled yet but is very close to the final static stress change around the ruptured part of the fault. In the second row of panels we show the results for a model that is slightly above critical,  $\kappa = 0.81$ . The rupture front in this model is almost steady state and will advance forever at sub-Rayleigh speed unless it encounters heterogeneities. In the third row  $\kappa = 1.1$  is just below the value of  $\kappa$  needed to produce a transition to supershear speeds. We observe a certain spread of the rupture front in the horizontal direction which is a clear indication that the rupture front is very close to the conditions that permit a super-shear transition but does not succeed. Finally, in the last row of Fig. 4, the non-dimensional number is 1.44, which is well above the minimum value needed for a transition to super-shear speeds. The rupture front in the in-plane direction has already jumped to super-shear speed and is close to steady state propagation so that rupture will continue at supershear speed forever. The slip rate panels (left in Fig. 4) show that the rupture front has a width

that is probably controlled by the initial size of the asperity as suggested by Madariaga and Cochard (1994) and Beroza and Mikumo (1996).

By a systematic study of models for different values of  $\kappa$  we find that rupture only occurs for values of  $\kappa$  greater than a certain value  $\kappa_c$ , the bifurcation point or critical point for the initiation of rupture in 3-D. By a systematic search we found that the critical point for rupture initiation in our model occurs for  $T_e = 0.52$ , so that  $\kappa_c = 0.60$ . The existence of this bifurcation is well known and several authors have interpreted it in terms of the radius of the minimum patch that may become unstable and generate dynamic rupture. Day (1982) computed the radius of this minimum patch in 3-D using Griffith criterion for the initiation of rupture from a circular crack. He found (equation 10 on page 1890):

$$R_c = \frac{7\pi}{24} \frac{\mu T_u D_c}{T_e^2},$$

from which we get an estimate of the critical value of  $\kappa$  at the bifurcation of  $\kappa_c = 0.996$ . The value we obtained from numerical experiments,  $\kappa_c = 0.66$ , is lower than that proposed by Day (1982). The reason is that Day studied the instability of a quasistatic circular crack loaded by an external stress field of amplitude  $T_e$ , while we are starting rupture by the instantaneous rupture of a circular patch loaded by a stress field of amplitude  $T_u = 1$ . There is clearly more energy available in our mode of rupture initiation than in Day's (1982) model. Rupture initiation is a very non-linear problem and we should not expect to obtain exactly the same critical number for different numerical experiments. We can compare the critical number we just found,  $\kappa_c = 0.66$ , with those computed by Andrews (1976b) for a 2-D in-plane fault. From the energy balance (Griffith's criterion) for a fault that is ready to break he found the critical half-width:  $L_c = 1/[\pi(1-\nu)] \mu T_u D_c / T_e^2$  where  $\nu$  is Poisson's modulus. This leads to a critical value  $\kappa_c = 1/[\pi(1-\nu)] \simeq 0.424$  for  $\nu = 1/4$ , the usual value of Poisson's ratio for crustal materials. For anti-plane rupture the minimum patch can be computed from Andrews's (1976a) expressions, he found  $\kappa_c = 1/\pi = 0.318$ . Thus, the critical number from our numerical experiments is bracketed by the analytical estimates for 2-D by Andrews and that of Day for a circular crack.

Thus, depending on the value of  $\kappa$ , a rupture propagates indefinitely at sub-Rayleigh speeds for  $0.66 < \kappa < 1.2$  or, after a some time, it jumps to supershear speed if  $\kappa > 1.2$ . Since there are no other parameters in this problem, this simple relation captures all the physics in this problem. It is interesting to note that as the rupture grows, the velocity concentration near the rupture front increases, but the stress concentration does not because rupture adjusts to exactly balance the energy flow to the slip-weakening zone with the energy release rate required for rupture to advance. This behavior is quite different from that of faults expanding at fixed rupture speed, like the self-similar model of Kostrov (1964). As shown by Andrews (1974) in 2-D, in 3-D there is also a small gap in the value of the parameter  $\kappa$  for which rupture propagates indefinitely at sub-shear speeds.

### Interpretation of the nondimensional parameter $\kappa$

Let us now try to understand the origin of the non-dimensional number  $\kappa$ . It is well-known in non-linear physics that, apart from shape factors, expressions like (7) can be derived from dimensional analysis. As discussed by Madariaga (1976), non-dimensional analysis of rupture in a uniform medium with uniform rupture resistance is relatively simple: displacement and slip scale like  $D \approx T_e / \mu \times L$ , where  $D$  is slip,  $T_e$  is the effective stress (a typical value of stress drop),  $L$  is a characteristic length scale, and  $\mu$  is the elastic rigidity. Energy release rate for such a model scales like  $E_r \approx T_e \times D = T_e^2 R / \mu$  and must be at least equal to the specific fracture energy  $G = \frac{1}{2} T_u D_c$  for rupture to propagate. From this extremely simple consideration we find the following non-dimensional control number:

$$\kappa = \frac{E_r}{G} \approx \frac{T_e^2 R}{\mu T_u D_c} \frac{R}{D_c}, \quad (8)$$

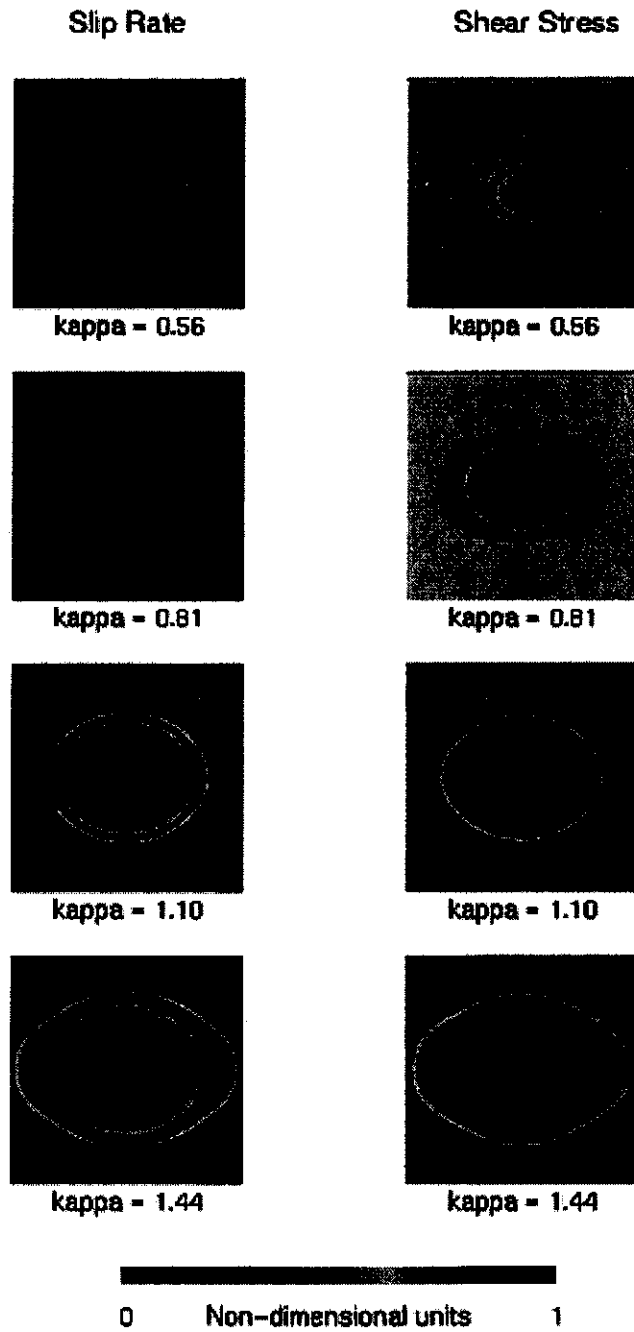


Figure 4: Snapshots of the slip rate (left) and shear stress change (right) on an unbounded 3-D fault where rupture starts from a circular, prestressed circular patch described in Fig. 2. From top to bottom the rows show ruptures at sub-critical, slightly super critical and super-critical values of the parameter  $\kappa$

# Rectangular Fault Model

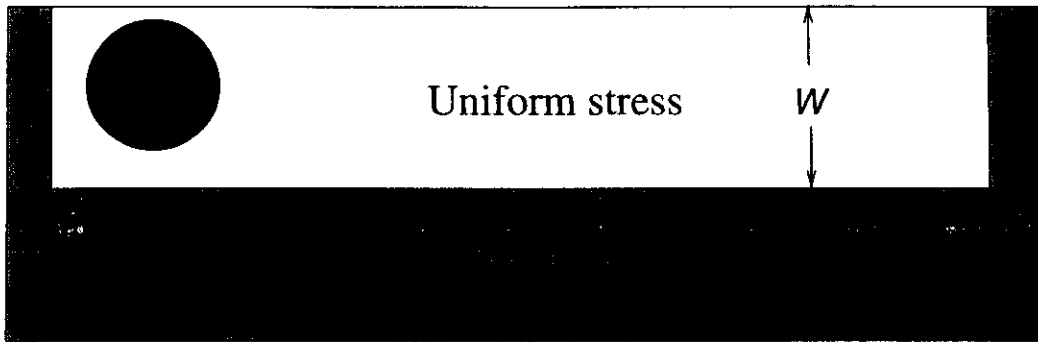


Figure 5: Shallow rectangular strike-slip dynamic shear fault studied in this paper.

where  $\approx$  means on the order of. Thus apart from numerical constants  $\kappa$  is the ratio of available strain energy to fracture energy. This nondimensional number controls the phenomenology of rupture as has been noted in some way or another by all the authors that have done numerical simulations of seismic ruptures. We realize now that  $\kappa_c$  defines a typical bifurcation. For  $\kappa < \kappa_c$  rupture does not grow beyond the initial asperity, while for  $\kappa > \kappa_c$  it grows indefinitely without ever stopping. This is a typical bifurcation of the behavior of faulting first noted by Griffith (1929).

## Shallow strike-slip rectangular fault

In a recent paper, Madariaga and Olsen (2000) studied two simple rectangular fault models and showed that the non-dimensional number  $\kappa$  controls rupture growth in 3-D. These models, a rectangular fault and a rectangular asperity, have a single external length scale: the fault width  $W$ .

In this section we study a very common rupture model that is more realistic than the unbounded ruptures described in the previous section. We consider a shallow rectangular vertical strike slip fault model limited above by a free surface and by an unbreakable barrier at the bottom of the seismogenic layer. The geometry of the model is shown in Figure 5. We assume that rupture is guided by the free surface and by a strong barrier of very large peak stress  $T_u = \infty$  that never breaks. For practical reasons of memory limitations in the computers, we also introduced barriers along the direction of faulting so that ruptures are limited to a finite zone and we do not run into numerical problems. We assume that the entire fault plane is subject to a constant “effective” shear stress  $T_e$  whose value we can change. The only additional ingredient in our model is the friction law defined above (3). Inside the fault of width  $W$ , rupture resistance is constant with  $D_c = 8$  and  $T_u = 1$ . Rupture starts from an initial asperity of radius  $R = 12$  that is large enough to initiate rupture. The fault width was fixed at  $W = 18$ . Thus we have a single free parameter  $T_e$  which we varied from 0.5 to 0.9. The shallow strike slip problem of Figure 5 has actually three length scales:  $R$ , the radius of the initial rupture patch,  $W$ , the width of the rectangular fault and  $D_c$  the slip weakening distance of the friction law. We assume that  $W > R > D_c$ .

The effect of the initial patch  $R$  was already studied in the previous section where we showed that the initiation of rupture is completely controlled by the non-dimensional number  $\kappa$ . Using the same arguments as used for the definition (7) we introduce the non-dimensional number

$$\kappa_w = \frac{T_e^2 W}{\mu T_u D_c}, \quad (9)$$

where we have replaced  $R$  by the width  $W$  of the fault. We will show that this non-dimensional number completely controls rupture propagation on the shallow rectangular fault.

In Figure 6 we show snapshots of the slip rate and shear stress fields on the fault at the same instant of time  $t = 120\Delta x/v_s$  for different values of the nondimensional number  $\kappa_w$  that varies from  $\kappa_w = 0.5625$  on the top panel to 1.44 at the bottom. In the top panel rupture has already stopped. The stress field shown on the right hand of the top panel is not completely settled yet but is very close to the final static stress change around the ruptured part of the fault. It shows that rupture started from the small circular asperity, propagated for some time along the fault plane and then spontaneously stopped because  $\kappa_w$  was not large enough to insure continuous propagation along the shallow fault. In the middle panels we show the results for a fault where  $\kappa_w$  is supercritical. From a series of numerical experiments we found that the critical value for  $\kappa_w$  was 0.76. For both  $\kappa_w = 0.81$  and  $\kappa_w = 1.10$  rupture propagates at sub-Rayleigh speeds along the longitudinal direction of the fault. The rupture front in this model is almost steady state and will simply continue rupture forever at this speed unless it encounters some stress or frictional heterogeneity in its way. The slip rate panel shows that the rupture front has a width that is probably controlled by the fault width as suggested by Day (1982). The stress field on the right hand side shows a peak in stress that runs slightly ahead of the rupture front. This is the shear wave front that shows that rupture is sub-shear in this case. Finally in the bottom two panels we show slip rate and stress change for a super-shear rupture. Here the rupture front has jumped ahead of the shear wave front and is close to a steady state. Rupture will continue forever at super-shear speeds until it runs into stress or strength heterogeneities.

Finally, at the bottom of Figure 6 we show a simulation where  $\kappa_w = 1.44$ . Rupture is now clearly supershear as can be seen from the spread of the rupture front as shown in the slip-rate panel on the left-hand side. Note again that seismic rupture propagation is a critical phenomenon that possesses two embedded bifurcations in the behavior of the system for a particular value of the nondimensional parameter  $\kappa$ .

For the shallow rectangular fault model we did not carry out a systematic exploration of the parameter space as we did for the rectangular fault in Madariaga and Olsen (2000) because we do not think it is necessary. In fact a shallow strike slip fault of width  $W$  that intercepts the free surface is similar to a long rectangular fault of width  $2W$  embedded in a full elastic space. The latter problem was studied in detail in Madariaga and Olsen (2000) where we showed that the qualitative behavior of rupture is controlled by the same value of  $\kappa_w$ . Thus all the results obtained earlier for a rectangular fault embedded in a full-space apply to the strike slip fault discussed here. Finally, as shown in Figure 6, we find again that when  $\kappa$  is sufficiently large ruptures grow initially at very high speeds and then jump to a speed higher than the shear wave velocity.

Although many authors have studied rupture conditions in the presence of asperities and barriers, most notably Das (1981), Das and Kostrov (1983, 1988), Kostrov and Das (1989) and Day (1982), we believe that this is the first time that conditions for rupture growth and arrest are systematically studied in a simple but realistic 3-D rupture model. Our results are entirely compatible with and extend those of Husseini et al (1978) who studied conditions for rupture of 2-D faults.

## Spontaneous rupture on a realistic fault: the Landers 1992 earthquake

Olsen et al (1997) studied a fully dynamic rupture model of the Landers earthquake of July 1992 that was based on the kinematic model inverted by Wald and Heaton (1994) from seismic and geodetic data. Recently, Peyrat et al (2000) inverted the accelerograms recorded around the Landers earthquakes by a trial-and-error method assuming that rupture resistance was uniform over the fault plane. The accelerograms were filtered at .5 Hz (2 s) so that the model contains wavelengths down to about 5 km.

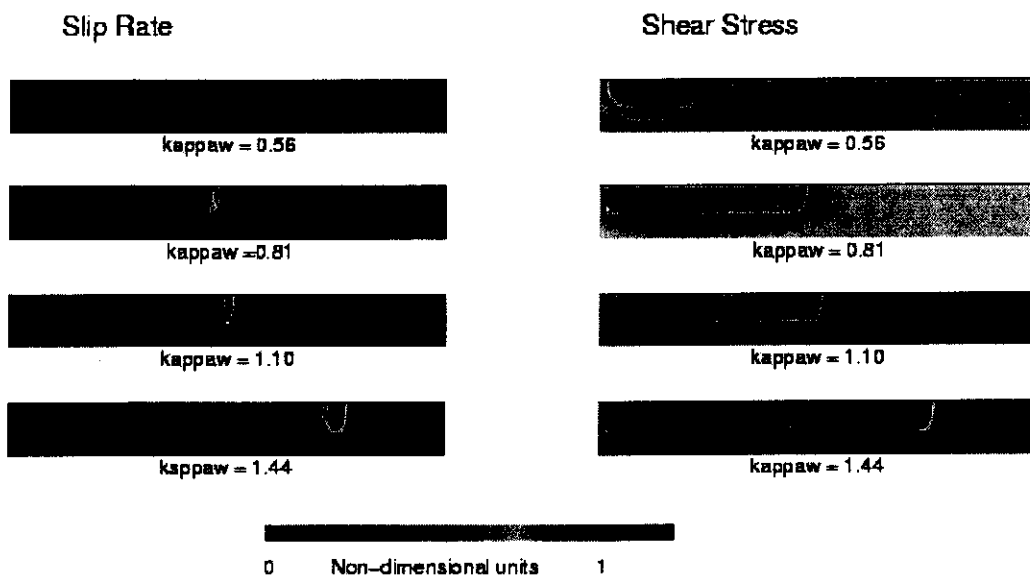


Figure 6: Snapshots of the slip rate (left) and shear stress (right) fields on a fault containing a very long and narrow asperity (yellow in the stress snapshots). Ruptures at (top) sub-critical, (middle) slightly super critical and (bottom) super critical values of the parameter  $\kappa$ .

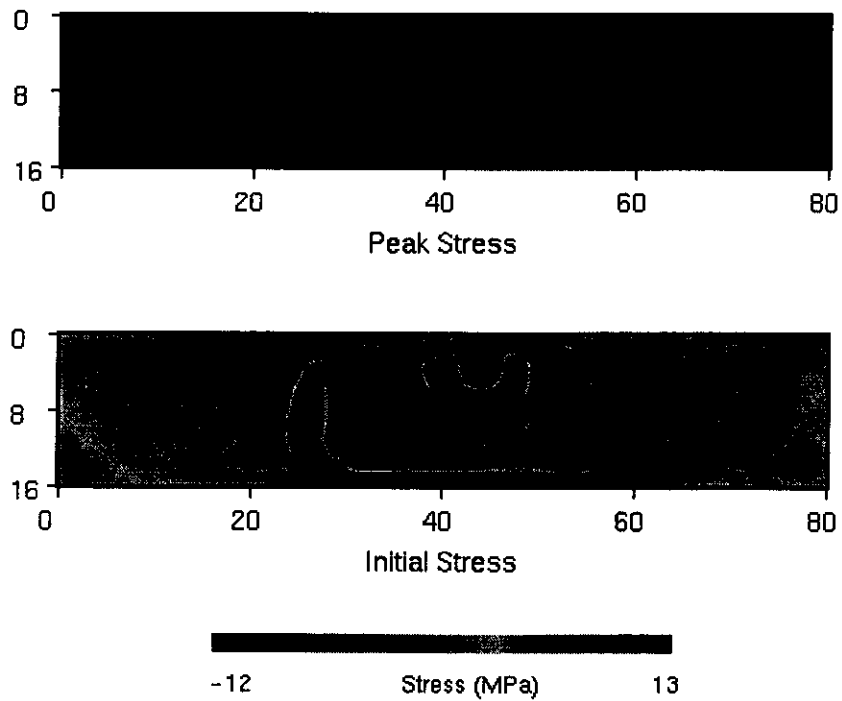


Figure 7: Initial conditions for the modeling of rupture in a realistic stress field inspired from the 28 June 1992. The initial stress field  $T_c$  is shown at the bottom as determined by Peyrat et al (2000) from the inversion of near field accelerograms. The picture at the top shows the peak stress distribution  $T_u$  for our numerical simulation. We initiated rupture from the circular area where we reduced  $T_u$  to a value low enough to initiate rupture. Slip weakening distance is fixed at  $D_c = 0.8$  m in our simulations.



Inversion was started using the initial stress field computed by Olsen et al (1997) from the slip model determined by Wald and Heaton (1994). With this initial stress field and the homogeneous friction model (3) a fully dynamic simulation of rupture was carried out. From the slip rate model determined by the simulation, synthetic seismograms were computed using the discrete wavenumber integration method (Bouchon, 1981, Coutant, personal communication, 1998). These synthetic accelerograms were then compared to observed ones. Inversion consisted then in adjusting the initial stress field in order to improve the fit between observed and computed accelerograms. Full details of the method are described in Peyrat et al (2000).

From the dynamic inversion we use the initial stress field shown in Figure 7. The range of variation of initial stress in this model is roughly from -12 MPa to 12 MPa. In addition to the initial stress field the only other assumption in the dynamic simulations was that friction (3) was uniform everywhere on the fault plane. In the simulations by Peyrat et al (2000) the peak stress was  $T_u = 12.5$  MPa and  $D_c = 0.8$  m, so that  $G = 5$  MJ/m<sup>2</sup>. This is a large value but on the order of magnitude of those quoted by Ohnaka and Shen (1999). For significantly larger values of  $G$ , the rupture would break the fault at super-shear speed leaving a uniform final stress field and a slip distribution that was completely different from that of Wald and Heaton (1994). For lower values of  $G$ , on the other hand, rupture would simply not propagate along the fault. Thus again we think that we are in the presence of a critical phenomenon.

We can now make a quick calculation of the value of  $\kappa$  for the model of Peyrat et al (2000). For that purpose we need an average value for the effective stress  $T_e$  which can be computed from the initial and final stress field. Although there are many ways to do this computation (see a full discussion by Madariaga, 1979), we obtain an average value close to  $T_e = 4$  MPa. The fault width was  $W = 16$  km. Finally we need is an estimate of the rigidity  $\mu$ . Although the structure near Landers is vertically heterogeneous we use the average value  $\mu = 3.37 \times 10^{10}$  Pa. Using these values we find a value of  $\kappa = 0.72$  for the Landers earthquake model. This is very close indeed to the critical value  $\kappa_c = 0.76$  we obtained above for the shallow rectangular strike-slip fault model. Thus it appears that on average rupture during the Landers earthquake was barely supercritical, this explains why the average rupture speed is also sub-shear. It must be pointed out however that the fault width is not the only length scale that controls rupture, the length scales that dominate the stress field of Figure 7 are clearly smaller than 15 km. All this seems to indicate that rupture in the Landers earthquake reproduces the general behavior of the kinematic model of Wald and Heaton only if  $\kappa$  is very close to critical. There are many corrections to apply to this calculation, but we believe that the main result will stand further scrutiny: rupture in the Landers earthquake was slightly super-critical, large enough to make the rupture grow but not large enough for rupture to become super-shear.

The fact that rupture is almost critical can be shown in another way. Careful study of rupture propagation in the initial stress field shown at the bottom of Figure 7 shows that rupture only propagates in regions of high stress that are sufficiently wide. It takes a very minor modification of the initial stress field to either stop it or to guide it into a different area of the fault. This observation was extensively used by Peyrat et al (2000) to invert for the initial stress field from accelerograms recorded in the near field.

In order to further illustrate our finding that the Landers rupture occurred under conditions that were very close to critical, we simulated ruptures for several values of the parameter  $\kappa$ . Unfortunately, the stress field is not very favorable to rupture initiation from the true hypocenter of Landers. This occurs because the stress field surrounding the initial patch is rather weak. We are so close to the critical condition at the hypocenter that it is much easier to stop rupture than to trigger it. For this reason we decided to study the possible initiation of rupture from another point on the fault that will better illustrate our ideas.

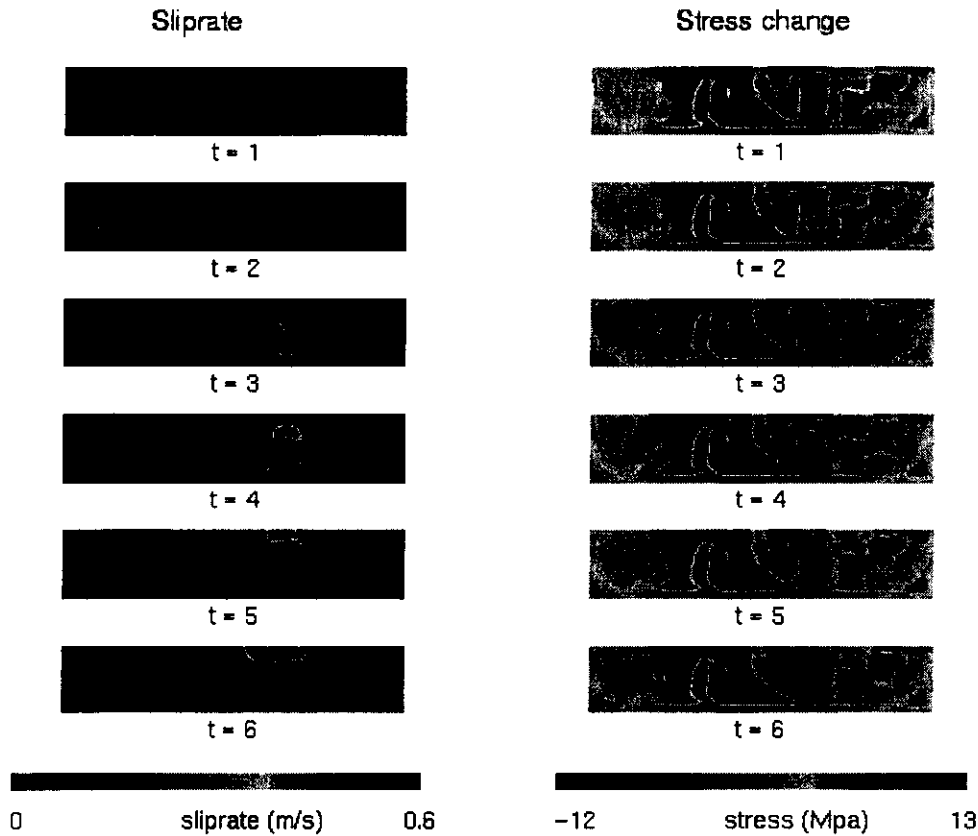


Figure 8: Snapshots at 1 s intervals of the slip rate field on the fault computed for a model inspired from the Landers 1992 earthquake. Rupture is triggered from a hypothetical initiation patch located as indicated in Fig. 7

In the simulations we started rupture from the patch shown in lighter color in Fig 7. This point is located inside an almost vertical column of high stress in the initial stress field. The width of this vertical zone or asperity is roughly 8 km. We start the rupture from a patch of radius  $R = 2$  km located at a depth of 9.8 km at a distance of 52 km from the end of the fault. Computation was done with a grid step  $\Delta x = 200$  m, a time step  $\Delta t = 0.0125$  s,  $T_u = 13$ MPa,  $D_c = 0.8$  m. The velocity structure and all other parameters were the same as those for the Landers earthquake simulation. In Figure 8 we show the longitudinal shear stress and slip rate fields at several successive instants of time. Only the initial instants of rupture simulation are shown here. What is striking is that slip rate is very localized inside the vertical asperity. It is clear that rupture is not controlled by the overall width of the fault but by the local length scales that in our case are clearly related to the initial stress distribution on the fault.

In order to define a critical parameter for our simulations of the Landers earthquake we have to define the proper width that goes into the nondimensional parameter. From our extensive experience in manipulating the initial stress in order to fit the observed accelerograms we know that the appropriate

length scale is neither the width of the fault nor the initial patch, but the local scale of the stress field. This was already proposed by Mikumo and Beroza (1994).

In conclusion the initial stress field controls rupture propagation very strongly. As long as rupture conditions are very close to critical, rupture extends following a relatively clear pattern of infiltration. It propagates into places where stress is high over large patches and avoids completely the zones where stresses are low. Only when conditions are very close to critical, the kinematics are similar to those determined by Wald and Heaton (1994), Cohee and Beroza (1994) or Cotton and Campillo (1995). If not, as first found by Olsen et al (1997), rupture jumps to supershear speeds and breaks the entire fault in a very short time.

### Discussion: where does the non-dimensional number come from?

Determining the exact value of the critical point of the non-dimensional number  $\kappa$  that controls the bifurcation in the behavior of a fault is a complex problem that will require the study of many models with variable geometries and complex stress distributions. The determination of such a number can be very complex as shown by Schmittbuhl and Vilotte (1997) who carried out an exhaustive study of the parameter space of the Burridge and Knopoff (1967) model. We believe that the general properties of rupture models near a critical point are more important than the exact value of the critical parameter  $\kappa_c$ . Although our experience is limited, numerical experiments with different geometries do not change the qualitative behavior of rupture as a function of  $\kappa$ . Actually, from discussion in the physics literature, the very fact that we have a bifurcation in the behavior of the system means that we must have a single non-dimensional control parameter that determines whether a rupture will grow or stop. In the rectangular barrier and asperity models the stress field is uniform so that we do not expect fractional powers; for this reason we successfully applied the simple dimensional analysis approach to find non-dimensional numbers (see, e.g. Landau and Lifshitz, 1959, page 63).

Inspired by the pionering work of Ida (1972) and Andrews (1976a,b), we have shown that the non-dimensional number  $\kappa$  arises from the competition between a measure of the strain energy released during rupture and the energy dissipated in fracture. It is thus a dynamic version of the Griffith criterion for the initiation of faulting. Our definition (7) implies that

$$\kappa \approx \Delta W/G. \quad (10)$$

For simple uniformly stressed models, we used results from Andrews (1976a,b) and Day (1982) to estimate the critical value of  $\kappa_c$  for 2-D fault geometries and for a circular fault. The values obtained range from 0.47 for antiplane cracks to 1.09 for circular ones. Our estimates for several simple models are also within this range of values, typically on the order of 0.75 when using the definition (7) where  $W$  is the half width or radius of the fault.

What is really interesting is that for the Landers earthquake, for which a number of authors have shown that it had a very complex slip and stress drop distribution, the numerical value of  $\kappa$  is very close to the critical values obtained for the different models we studied. This suggests to us that rupture during the Landers earthquake occurred under general conditions that were very close to criticality. Actually if one uses the values generally quoted for stress drops of about 3 MPa, standard values of rigidity in the crust ( $\simeq 30$  GPa), and energy release rates on the order of 3 GPa often quoted in the literature, we get  $\kappa \simeq 0.5$ , very close indeed to the critical values for  $\kappa$ .

Although we must warn that for more general models with fractal distributions of stress and fracture resistance  $G$ , we expect that the expression for  $\kappa$  may include fractional powers of non-dimensional ratios of stresses and linear dimensions.

We can now speculate on the behavior of active faults in the earth. We have seen from these simple examples that the essential requirement for rupture to grow is that  $\kappa > \kappa_c$  where the critical value

of  $\kappa$  depends on the geometry of the problem but is on the order of 1. Once  $\kappa$  becomes much larger than critical, ruptures tend to become super-shear very quickly, but this is rarely observed in nature. Why is it so? We believe that ruptures are in general sub-shear because faults always stay close to the critical condition. The reason may be very simple: as soon as the conditions for rupture in an area of the fault are fulfilled a rupture will occur, unloading the fault. When the system is loaded again to criticality another earthquake will occur and so on. The size of these earthquakes is not determined by the load but by the connectivity of the stress or rupture resistance field. In other words the earthquake will go as far as the stress field permits! Under special circumstances stress can be high and the fault remains in supercritical condition. Only in those exceptional circumstances will super-shear speeds be observed (Archuleta, 1984, Olsen et al, 1997). The normal behavior for earthquakes is to break under critical conditions at speeds below the shear wave speed. This eliminates the very old dilemma of why do earthquakes stop, and why there are earthquakes of vastly different sizes on the same fault segment.

## Conclusions

We have carefully studied rupture growth in a simple flat fault embedded in a homogeneous elastic medium of rigidity  $\mu$ . It emerges from our studies that rupture is controlled by a non-dimensional number  $\kappa = T_e^2 / \mu T_u \times L / D_c$  where  $L$  is a characteristic size of the stress field, for instance the patch (asperity) radius or the width of the fault or asperity,  $T_e$  is a characteristic stress drop on the fault and  $T_u \times D_c$  is a measure of energy release rate on the fault.

We then computed  $\kappa$  for the dynamic simulation of the 1992 Landers earthquake models of Olsen et al (1997) and Peyrat et al (2000) that were based on the Wald and Heaton (1994) kinematic model. From a rough estimate we found that  $\kappa = 0.76$  was slightly higher than the critical value  $\kappa_c = 0.72$ , implying that the Landers earthquake rupture occurred under conditions that were almost critical. Several additional evidences in favor of criticality were examined, leading to the hypothetical suggestion that earthquake ruptures occur soon after the stress distribution on the fault becomes critical and that faults rarely stay in a metastable state that would allow large supercritical states on the fault.

In our analysis so far we have assumed uniform rupture resistance (constant  $T_u$  and  $D_c$ ). All the complexity in our models arises from the heterogeneity of the initial stress. As important as stress heterogeneity is probably the small scale geometry of faulting. However, taking it into account in fault models is difficult because most of the observations of fault rupture are still limited to the range of frequencies of less than 1 Hz or about 3 km wavelength. This is too coarse a resolution to observe effects of complex geometry other than major fault segmentation as in Landers or Kobe. High frequency seismic radiation is probably the only source of information about small scale geometry.

## Acknowledgments

We thank J.R. Rice for very useful discussions concerning the origin of the non-dimensional number  $\kappa$ . Computations for this study were carried out in the parallel computer of Département de Modélisation Physique et Mathématique of Institut de Physique du Globe de Paris. R. Madariaga and S. Peyrat were supported by the Environment Program of the European Community under project SGME and by INSU-CNRS under contract from the Programme National des Risques Naturels. K. Olsen's work was supported by the Southern California Earthquake Center (SCEC). SCEC is funded by NSF Cooperative Agreement EAR-8920136 and USGS Cooperative Agreements 14-08-0001-A0899 and 1434-HQ-97AG01718. This is ICS contribution 0345-93EQ and SCEC contribution number 534. }

- ANDREWS, J. (1976a): Rupture propagation with finite stress in antiplane strain, *J. Geophys. Res.*, **81**, 3575-3582.
- ANDREWS, J. (1976b): Rupture velocity of plane strain shear cracks, *J. Geophys. Res.*, **81**, 5679-5687.
- ANDREWS, J. (1985): Dynamic plane-strain shear rupture with a slip-weakening friction law calculated by a boundary integral method, *Bull. Seismol. Soc. Am.*, **75**, 1-21.
- ARCHULETA, R. (1984): A faulting model for the 1979 Imperial Valley earthquake, *J. Geophys. Res.*, **89**, 4559-4585.
- BAK, P., C. TANG and K. WIESENFELD (1987): Self-organized criticality, *Phys. Rev.*, **A38**, 364.
- BEROZA, G., and T. MIKUMO (1996): Short slip duration in dynamic rupture in the presence of heterogeneous fault properties, *J. Geophys. Res.*, **101**, 22449-22460.
- BOUCHON, M. (1997): The state of stress on some faults of the San Andreas system as inferred from near-field strong motion data, *J. Geophys. Res.*, **102**, 11731-11744.
- BOUCHON, M. (1981): A simple method to calculate Green's functions for elastic layered media, *Bull. Seismol. Soc. Am.*, **71** 959-971.
- BURRIDGE, R., G. KOHN and L.B. FREUND (1979): The stability of rapid mode II shear crack with finite cohesive friction, *J. Geophys. Res.*, **85**, 2210-2222.
- BURRIDGE, R., and L. KNOPOFF (1967): Model and theoretical seismicity, *Bull. Seismol. Soc. Am.*, **67**, 341-371.
- CARLSON, J., and J. LANGER (1989): Mechanical model of an earthquake fault, *Phys. Rev. A*, **40**, 6470-6484.
- COCHARD, A., and R. MADARIAGA (1994): Dynamic faulting under rate-dependent friction, *Pageoph*, **142**, 419-445.
- COCHARD, A., and R. MADARIAGA (1996): Complexity of seismicity due to highly rate-dependent friction, *J. Geophys. Res.*, **101**, 25321-25336.
- COHEE, B., and G. BEROZA (1994): Slip distribution of the 1992 Landers earthquake and its implications for earthquake source mechanics, *Bull. Seis. Soc. Am.*, **84**, 692-712.
- COTTON, F., and M. CAMPILLO (1995): Frequency domain inversion of strong motions: application to the 1992 Landers earthquake, *J. Geophys. Res.*, **100**, 3961-3975.
- DAS, S. (1981): Three-dimensional spontaneous rupture propagation and implications for the earthquake source mechanism, *Geophys. J. Roy. astr. Soc.*, **67**, 375-393.
- DAS, S., and K. AKI (1977): A numerical study of two-dimensional spontaneous rupture propagation, *Geophys. J. Roy. astr. Soc.*, **50**, 643-668.
- DAS, S., and B. KOSTROV (1983): Breaking of a single asperity: Rupture process and seismic radiation. *J. Geophys. Res.*, **88**, 4277-4288.

- DAS, S., and B. KOSTROV (1988): An investigation of the complexity of the earthquake source time function using dynamic faulting models. *J. Geophys. Res.*, **93**, 8035-8050.
- DAY, S. (1982): Three-dimensional simulation of spontaneous rupture: the effect of non-uniform prestress, *Bull. Seismol. Soc. Am.*, **72**, 1881-1902.
- DIETERICH, J. (1978): Time-dependent friction and the mechanics of stick-slip, *Pageoph*, **116**, 790-806.
- FREUND, L.B. (1989): *Dynamic Fracture Mechanics*. Cambridge University Press, Cambridge, U.K.
- FUKUYAMA, E., and R. MADARIAGA (1998): Rupture dynamics of a planar fault in a 3-D elastic medium: Rate- and slip-weakening friction, *Bull. Seismol. Soc. Am.*, **88**, 1-17.
- GRIFFITH, A. A. (1929): The phenomenon of rupture and flow in solids, *Phil. Trans. Roy. Soc. London, A* **221**, 163-198.
- HARRIS, R., and S. DAY (1993): Dynamics of fault interaction: parallel strike-slip faults, *J. Geophys. Res.*, **98**, 4461-4472.
- HEATON, T. (1990): Evidence for and implications of self-healing pulses of slip in earthquake rupture, *Phys. Earth. Planet. Int.*, **64**, 1-20.
- HUSSEINI, M.I., D.B. JOVANOVIĆ, M.J. RANDALL and L.B. FREUND (1975): The fracture energy of earthquakes, *Geophys. J. Roy. Astr. Soc.*, **43**, 367-385.
- IDA, Y. (1972): Cohesive force across the tip of a longitudinal-shear crack and Griffith's specific surface energy, *J. Geophys. Res.*, **77**, 3796-3805.
- IDE, S., and M. TAKEO (1997): Determination of the constitutive relation of fault slip based on wave analysis, *J. Geophys. Res.*, **102**, 27379-27391.
- KANAMORI, H. and G.S. STEWART (1978): Seismological aspects of the Guatemala earthquake of February 4, 1976, *J. Geophys. Res.*, **83**, 3427-3434.
- KOSTROV, B. (1964): Self-similar problems of propagation of shear cracks, *J. Appl. Math. Mech.*, **28**, 1077-1087.
- KOSTROV, B.V., and S. DAS (1989): *Principles of Earthquake Source Mechanics*, Cambridge University Press, Cambridge, U.K.
- LANDAU, L., and E. LIFSHITZ (1959): *Fluid Mechanics*, Pergamon Press, London.
- MADARIAGA, R. (1976): Dynamics of an expanding circular fault, *Bull. Seismol. Soc. Am.*, **66**, 639-667.
- MADARIAGA, R. (1979): On the relation between seismic moment and stress drop in the presence of stress and strength heterogeneity, *J. Geophys. Res.*, **84**, 2243-2250.
- MADARIAGA, R., K.B. OLSEN and R.J. ARCHULETA (1998): Modeling dynamic rupture in a 3-D earthquake fault model, *Bull. Seismol. Soc. Am.*, **88**, 1182-1197.

- MADARIAGA, R., and K.B. OLSEN (2000): Criticality of rupture dynamics in three dimensions, *Pageoph* in press.
- MIKUMO, T., and T. MIYATAKE (1995): Heterogeneous distribution of dynamic stress drop and relative fault strength recovered from the results of waveform inversion, *Bull. Seismol. Soc. Am.*, **85**, 178-193.
- OKUBO, P. (1989): Dynamic rupture modeling with laboratory-derived constitutive relations, *J. Geophys. Res.* **94**, 12321-12335.
- OHNAKA, M., and L-F. SHEN (1999): Scaling of rupture process from nucleation to dynamic propagation: implications of geometric irregularity of the rupturing surfaces, *J. Geophys. Res.*, **104**, 817-844.
- OLSEN, K.B., R. MADARIAGA and R.J. ARCHULETA (1997): Three dimensional dynamic simulation of the 1992 Landers earthquake, *Science*, **278**, 834-838.
- PEYRAT, S., K.B. OLSEN and R. MADARIAGA (2000): Dynamic modeling of the 1992 Landers earthquake, submitted to *J. Geophys. Res.*.
- RICE, J.R. (1993): Spatio-temporal complexity of slip on a fault, *J. Geophys. Res.*, **88**, 9885-9907.
- RICE, J., and Y. BEN-ZION (1996): Slip complexity in earthquake fault models, *Proc. Natl. Acad. Sci. USA*, **93**, 3811-3818.
- SATO, T., and T. HIRASAWA (1973): Body wave spectra from propagating shear cracks, *J. Phys. Earth*, **21**, 415-431.
- ROSAKIS, A.J., O. SAMUDRALA and D. COKER (1999): Cracks faster than the shear wave speed, *Science*, **284**, 1337-1340.
- SCHMITTBUHL, J., J.P. VILOTTE and S. ROUX (1996): A dissipation-based analysis of an earthquake fault model, *J. Geophys. Res.*, **101**, 27741-27764.
- SHAW, B., and J.R. RICE (2000): Existence of continuum complexity in the elastodynamics of repeated fault ruptures, *J. Geophys. Res.* in press.
- VIRIEUX, J., and R. MADARIAGA (1982): Dynamic faulting studied by a finite difference method, *Bull. Seismol. Soc. Am.*, **72**, 345-369.
- WALD, D., and T. HEATON (1994): Spatial and temporal distribution of slip for the 1992 Landers, California earthquake, *Bull. Seismol. Soc. Am.*, **84**, 668-691.

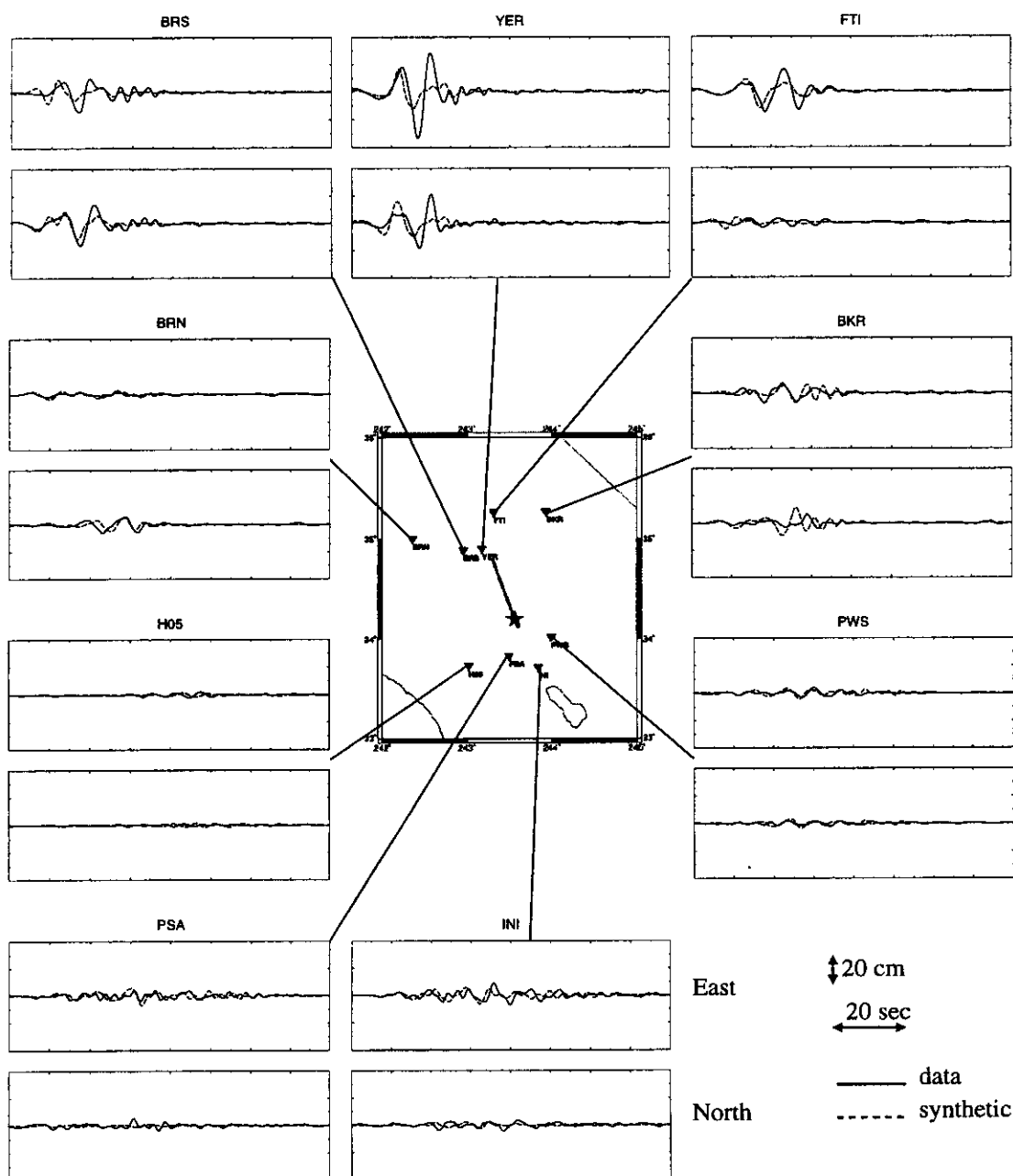


**Figure 10.** Comparison between observed ground displacements and those obtained for the starting model of the Landers 1992 earthquake [Olsen *et al.*, 1997]. For each station the upper trace is the east-west component of displacement and the bottom trace is north-south component. The time window is 80 seconds, and the amplitude scale is the same for each station.



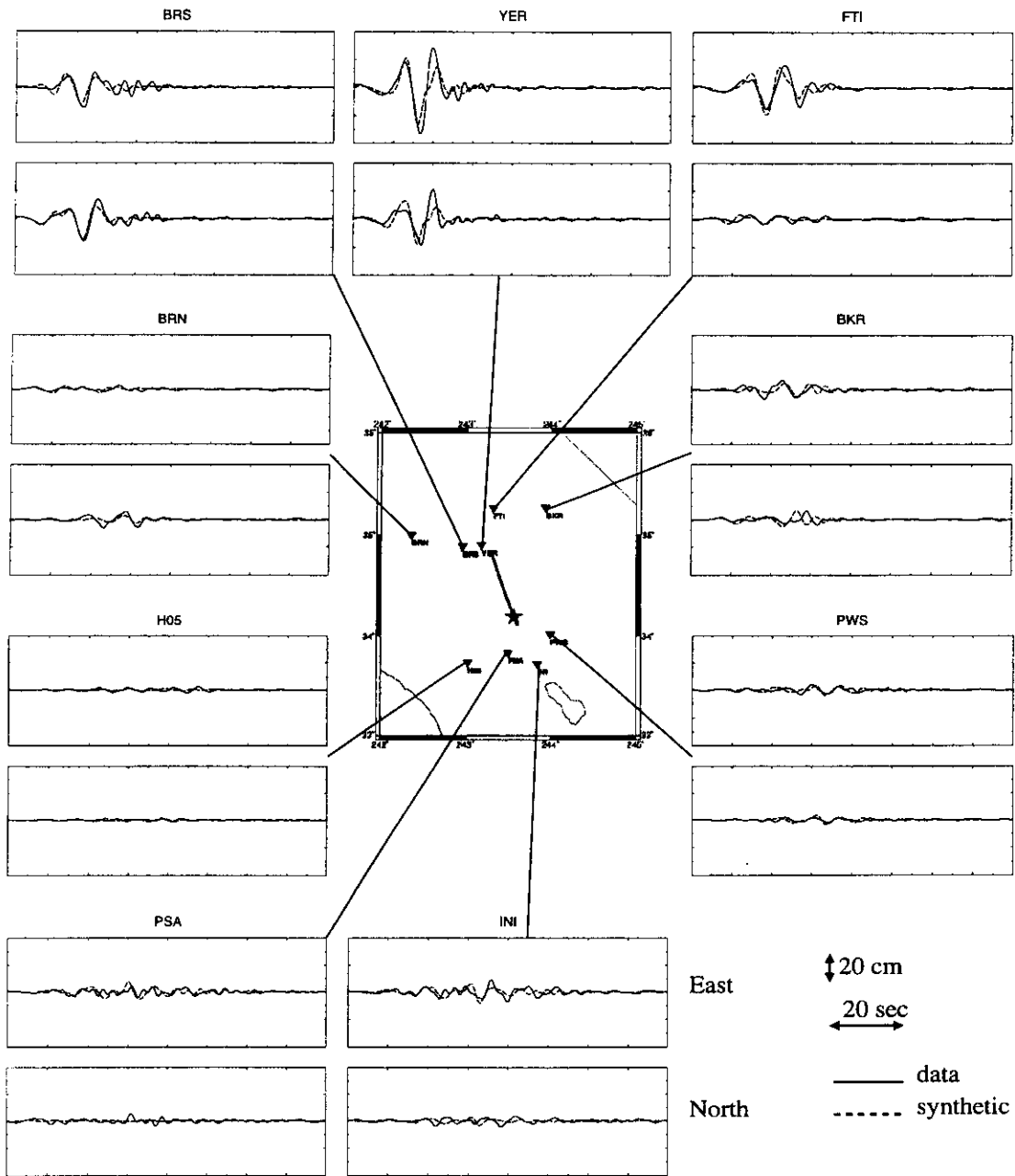


Figure 11. Same as Fig 10, but for our preferred dynamic model.

## Tables

**Table 1.** One-dimensional model used in numerical modeling.  $V_p$  and  $Q_p$  are the P-wave velocity and quality factor, respectively,  $V_s$  and  $Q_s$  are the S-wave velocity and quality factor, respectively, and  $\rho$  is the density of the medium.

Depth (km)	$V_p$ (km/s)	$V_s$ (km/s)	$\rho$ ( $g/cm^3$ )	$Q_p$	$Q_s$
0	3.8	1.98	2.30	100	30
1.5	5.5	3.15	2.60	600	300
4	6.2	3.52	2.70	600	300
26	6.8	3.83	2.87	600	300
32	8.0	4.64	3.50	600	300

**Table 2.** Stations from CDMG California Strong Motion Program (California Division of Mines and Geology) used in dynamic modeling.

Station Name	Station location	Epicentral Distance (km)	Closest Distance to Fault (km)
BKR	Baker	123.9	85
BRN	Boron	142.5	99.3
BRS	Barstow	94.7	44.4
FTI	Fort Irwin	120.9	66.8
H05	Hemet Fire Station	72.6	70.1
INI	Indio	59.7	54.3
PSA	Palm Springs	41.8	37.1
PWS	Twentynine Palms	44.2	40.5
YER	Yermo	85.8	31